

Supplementary informations

Multi-resonance TADF non-conjugated copolymer with near-unity photoluminescence quantum yield for efficient solution-processed OLEDs

Rundong Tian,^a Zhi Yang,^a Zihan Wang,^a Jinxin Dong,^a Weihao Li,^a Guangfu Li^{*a} and Hui Xu^{*a}

^aKey Laboratory of Functional Inorganic Material Chemistry (Chinese Ministry of Education),
School of Chemistry and Material Science, Heilongjiang University, 74 Xuefu Road, Harbin
150080, China

Correspondence should be addressed to hxu@hlju.edu.cn (H. Xu).

Contents

1. Experimental section	S2
2. ¹ H NMR spectra of PBN _x DPOT _y	S5
3. Thermogravimetric analysis	S7
4. CV results	S7
5. Frontier molecular orbits	S8
6. Photophysics properties of PBN _x DPOT _y	S9
7. EL performance of PBN _x DPOT _y -zw%	S11
8. References	S12

1. Experimental section

Materials and instruments

^1H NMR spectra were recorded using a Varian Mercury plus 400NB spectrometer relative to tetramethylsilane (TMS) as internal standard. Absorption and photoluminescence (PL) emission spectra of the target compound were measured using a SHIMADZU UV-3150 spectrophotometer and a SHIMADZU RF-5301PC spectrophotometer, respectively. Thermogravimetric analysis (TGA) and differential scanning calorimetry (DSC) were performed on Shimadzu DSC-60A and DTG-60A thermal analyzers under nitrogen atmosphere at a heating rate of $10\text{ }^\circ\text{C min}^{-1}$. Cyclic voltammetric (CV) studies were conducted using an Eco Chemie B. V. AUTOLAB potentiostat in a typical three-electrode cell with a glassy carbon working electrode, a platinum wire counter electrode, and a silver/silver chloride (Ag/AgCl) reference electrode. All electrochemical experiments were carried out under a nitrogen atmosphere at room temperature in dichloromethane. Phosphorescence spectra were measured in dichloromethane using an Edinburgh FLS 1000 fluorescence spectrophotometer at 77 K cooling by liquid nitrogen with a delay of 300 μs using Time-Correlated Single Photon Counting (TCSPC) method with a microsecond pulsed Xenon light source for 10 μs -10 s lifetime measurement, the synchronization photomultiplier for signal collection and the Multi-Channel Scaling Mode of the PCS900 fast counter PC plug-in card for data processing. The MR-TADF dye doped films (100 nm) were prepared through solution process for optical analysis. Photoluminescence quantum yields (PLQY, ϕ_{PL}) of these films were measured through a lab sphere ($\phi = 6''$) integrating sphere coated by Benflect with efficient light reflection in a wide range of 200-1600 nm, which was integrated with FLS 1000. The absolute η_{PL} determination of the sample was performed by two spectral (emission) scans, with the emission monochromator scanning over the Rayleigh scattered light from the sample and from a blank substrate. The first spectrum recorded the scattered light and the emission of the sample, and the second spectrum contained the scattered light of Benflect coating. The integration and subtraction of the scattered light parts in these two spectra arrived at the photon number absorbed by the samples (N_a); while, integration of the emission of the samples to calculate the emissive photon number (N_e). Then, the absolute ϕ_{PL} can be estimated according to the equation of $\eta_{\text{PL}} = N_e/N_a$. Spectral correction (emission arm) was applied to the raw data after background subtraction, and

from these spectrally corrected curves the quantum yield was calculated using a F900 software wizard. The absolute PLQY was determined through three independent measurements, with a measurement uncertainty of $\pm 0.15\%$.

Synthesis

All the reagents used for synthesis were purchased from Alfa and Sinopharm Chemical Reagent Co., Ltd, and used without further purification.

In Ar, 0.4135 g of diphenyl(4-phenyl-6-(4-vinylphenyl)-1,3,5-triazin-2-yl) phosphine oxide (ST, 0.9 mmol) and 0.0743 g DBNCz (ST, 0.1 mmol) and 0.0033g AIBN (ST, 0.02 mmol) dissolved in anhydrous THF (1.0 mL). The solution was warmed to 80 °C, then the mixture was stirred for 48 h. After the reaction is completed, the mixtures are slowly dropped into methanol that has been cooled to 0 °C in advance and stirred vigorously. The settled mixture is immediately subjected to vacuum filtration under reduced pressure. Then, the mixture was purified in methanol by Soxhlet extraction for 72 hours, followed by suction filtration and drying, and finally the product was obtained. After purification, yellowish-green powder was obtained with a moderate yield of 98%. $^1\text{H NMR}$ (TMS, 400 MHz, CDCl_3) δ [ppm] = 8.40 (s, 1H), 8.13 (s, 1H), 7.03 (s, 31H), 6.61 (s, 25H), 6.09 (s, 20H), 2.35 (s, 2H), 1.94 (s, 4H), 1.56 (s, $J = 10.0$ Hz, 16H).

Precise control of number-average molecular weight (M_n) and polydispersity index (PDI) requires strict optimization of AIBN initiator dosage. The polymer chain length exhibits an inverse relationship with AIBN concentration, longer target polymer chains need low concentration of initiator. The PDI typically decreases with of the concentration of AIBN.

Gaussian calculations

DFT computations were carried out with different parameters for structure optimizations and vibration analyses. The ground state in vacuum was optimized by the restricted and unrestricted formalism of Beck's three-parameter hybrid exchange functional[1] and Lee, and Yang and Parr correlation functional[2] B3LYP/6-31G(d,p), respectively. The fully optimized stationary points were further characterized by harmonic vibrational frequency analysis to ensure that real local minima had been found without imaginary vibrational frequency. The total energies were also corrected by zero-point energy both for the ground state and triplet state. The contours were visualized with Gaussview 5.0. All computations were performed using the Gaussian 09 package.[3]

OLED fabrication

All the materials were purchased from Xi'an Polymer Light Technology Corp. ITO substrate was cleaned and loaded into a deposition chamber. Firstly, the PEDOT:PSS layer (mixed with deionized water in a 1:1 ratio) was prepared using a coater at a rotational speed of 2000r/ minute. Then, it was annealed at 120 °C for 15 minutes, cooled for 10 minutes to return to room temperature, and then the PVK layer (dissolved in dry chlorobenzene) was continued to be spin-coated at a rotational speed of 3000r/min. Anneal at 50 °C for 10 minutes, cool for 10 minutes to return to room temperature, and then continue to spin coat the EML layer (dissolved in dry chlorobenzene). The rotational speed is 3000r/min. Annealing is carried out at 50 °C for 10 minutes. After cooling for 10 minutes and returning to room temperature, it is placed in deposition chamber. Fabricated layer-by-layer through evaporation at a pressure below 4×10^{-4} Pa. Deposition rates are 0.1-0.2 nm s⁻¹ for organic layers, 0.1 nm s⁻¹ for LiF (1 nm) and 0.6 nm s⁻¹ for Al (100 nm). The dimensionalities of each pixel were 0.3×0.3 cm². After deposition, the devices were transferred to glove box and encapsulated with glass cover slips and epoxy glue. The spectra and CIE coordinates were measured using a PR655 spectra colorimeter, under ambient conditions. The current density-voltage-brightness curves were measured using a Keithley 4200 source meter and a calibrated silicon photodiode. EL transient spectra were measured with Edinburgh FLS1000 equipped with a Tektronix AFG3022G function generator. The driving voltage was 5 V. The pulse width was 20 μs.

2. ^1H NMR spectra of $\text{PBN}_x\text{DPOT}_y$

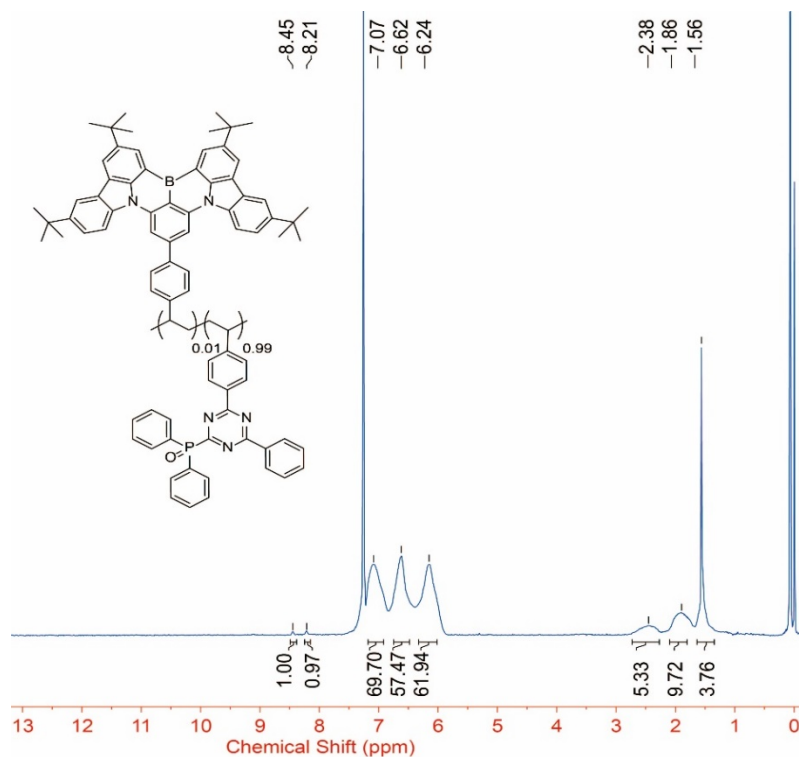


Figure S1. ^1H NMR spectrum of $\text{PBN}_1\text{DPOT}_{99}$ in CDCl_3 .

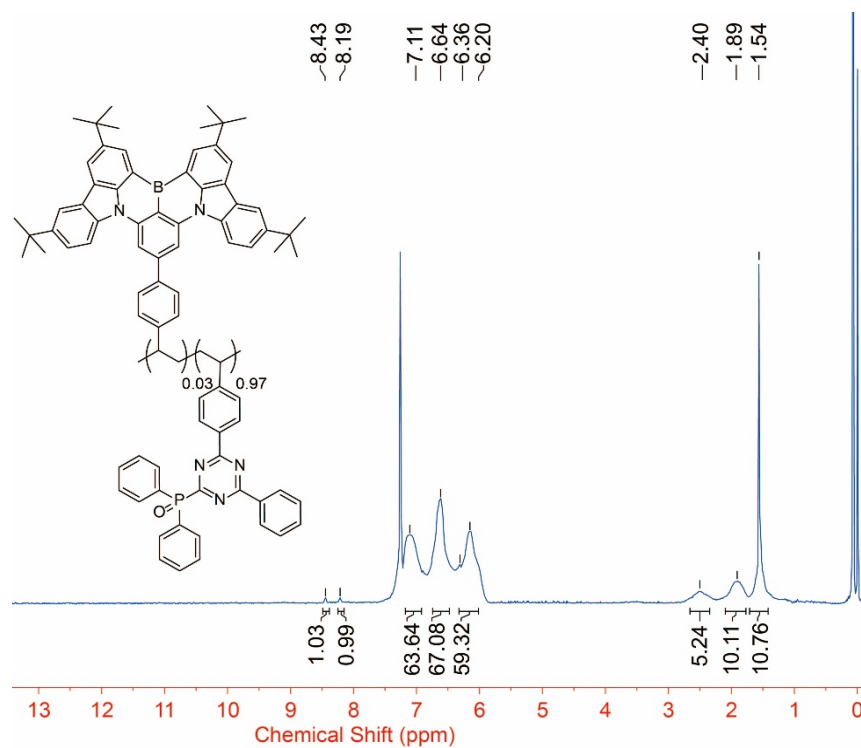


Figure S2. ^1H NMR spectrum of $\text{PBN}_3\text{DPOT}_{97}$ in CDCl_3 .

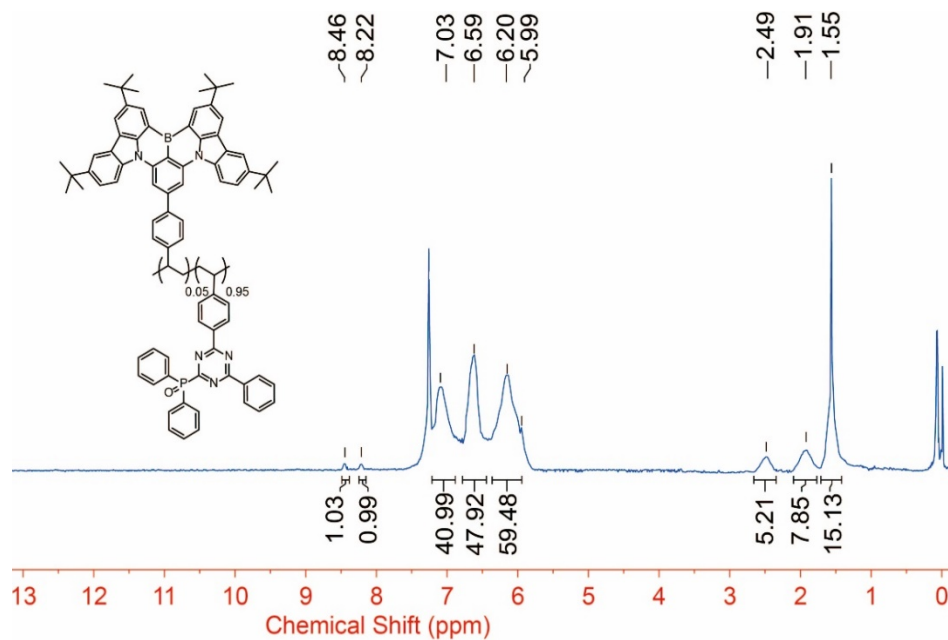


Figure S3. ¹H NMR spectrum of PBN₅DPOT₉₅ in CDCl₃.

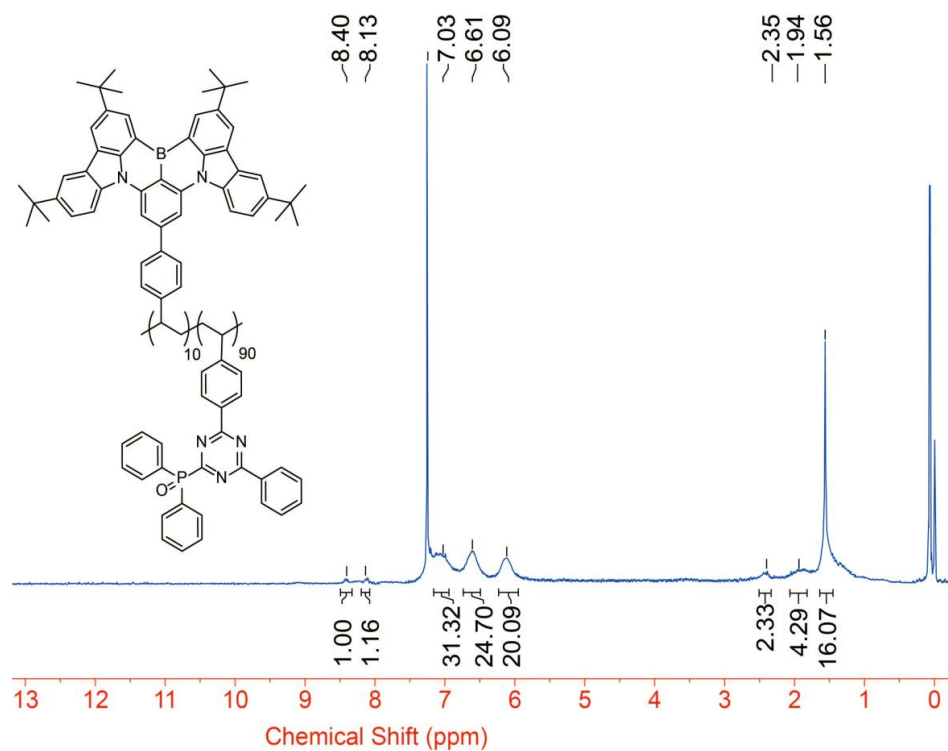


Figure S4. ¹H NMR spectrum of PBN₁₀DPOT₉₀ in CDCl₃.

3. Thermogravimetric analysis

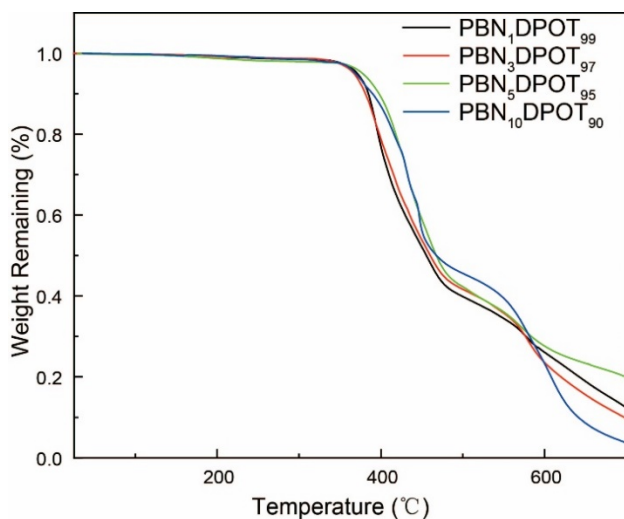


Figure S5. Thermogravimetric analysis (TGA) curves of $\text{PBN}_x\text{DPOT}_y$.

4. CV results

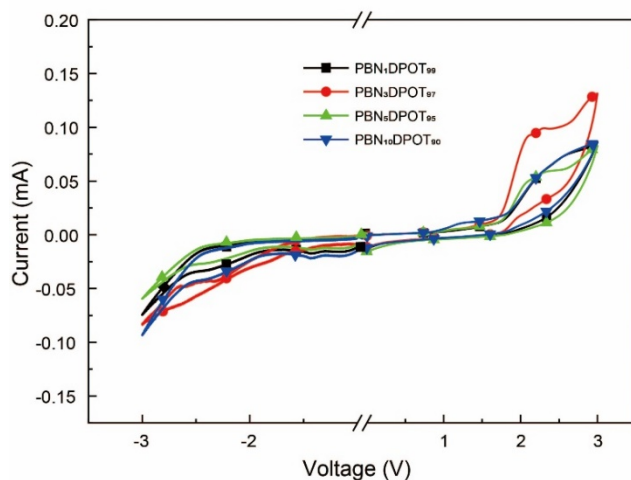


Figure S6. CV curves of $\text{PBN}_x\text{DPOT}_y$.

Table S1. The oxidation and reduction potentials of the $\text{PBN}_x\text{DPOT}_y$

	$\text{PBN}_1\text{DPOT}_{99}$	$\text{PBN}_3\text{DPOT}_{97}$	$\text{PBN}_5\text{DPOT}_{95}$	$\text{PBN}_{10}\text{DPOT}_{90}$
E_{ox} (V)	2.22	2.10	2.07	2.02
E_{red} (V)	-1.76	-1.77	-1.90	-1.93

5. Frontier molecular orbitals

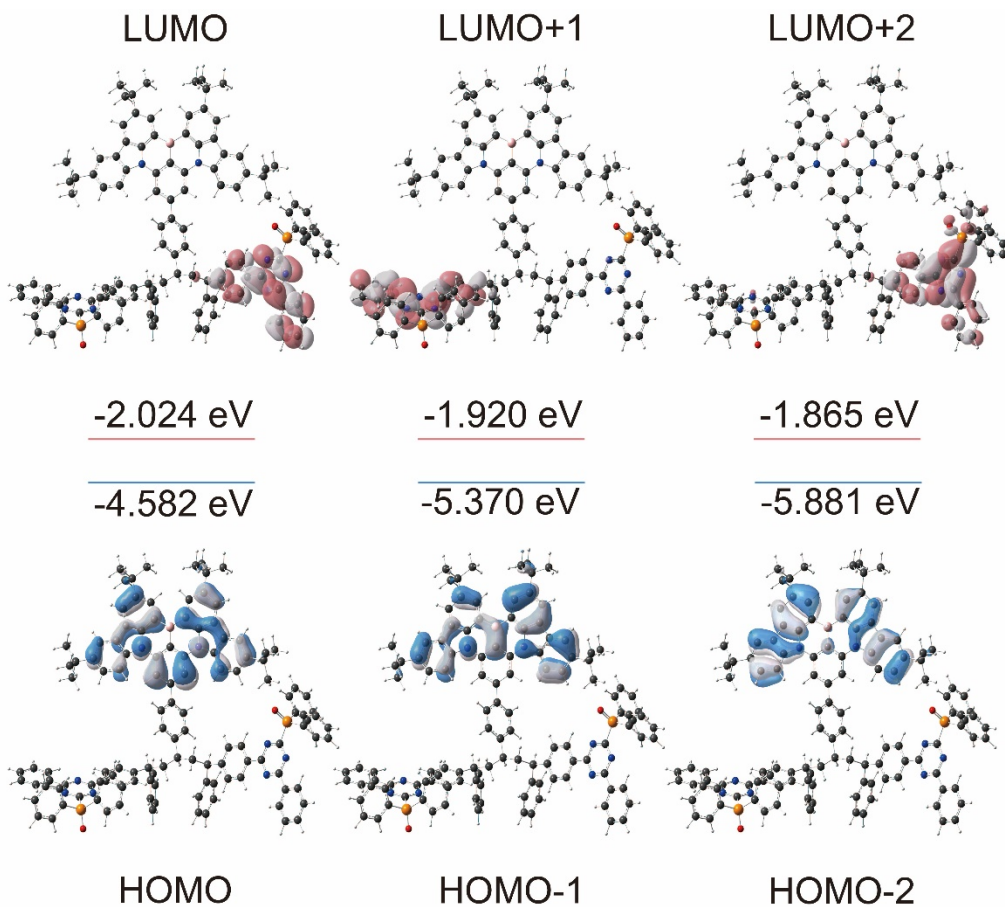


Figure S7. Contours of the HOMO, HOMO-1, HOMO-2 and LUMO, LUMO+1, LUMO+2 of PBN_xDPOT_y for ground state and corresponding energy levels.

6. Photophysics properties of PBN_xDPOT_y

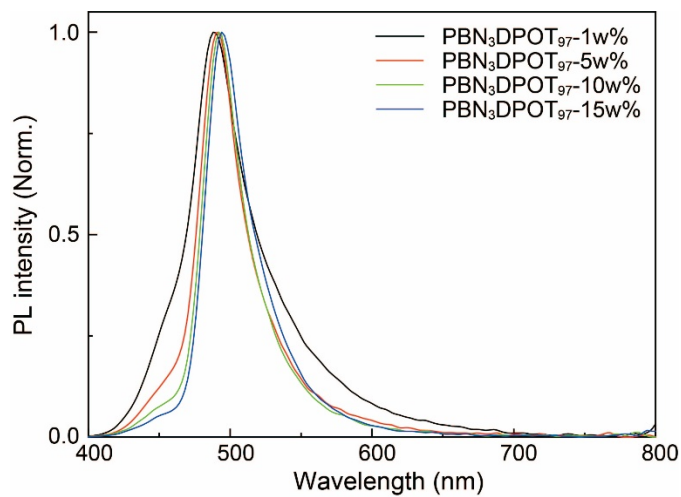


Figure S8. Photoluminescence spectra of PBN₃DPOT₉₇ doped with CzAcSF host materials in different doping concentrations (1, 5, 10 and 15%).

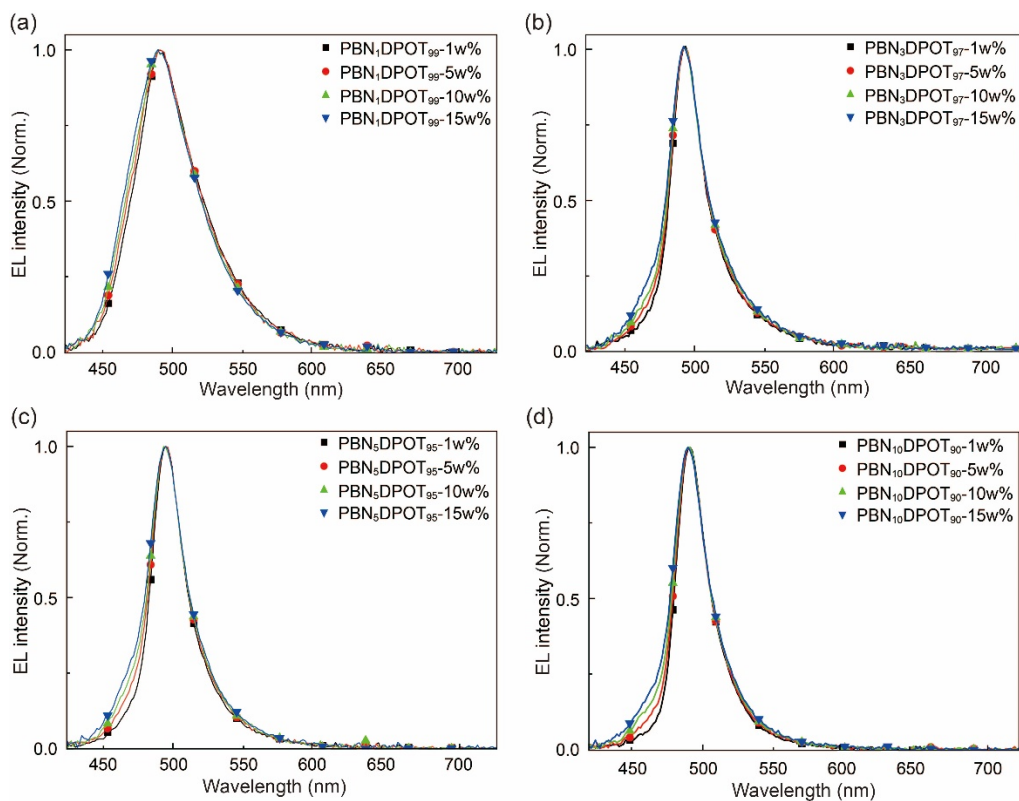


Figure S9. Electroluminescence spectra of PBN_xDPOT_y emitter (x = 1, 3, 5 and 10; y = 99, 97, 95 and 90).

Table S2. The number-average molecular weight, weight average molecular weight and PDI of the **PBN_xDPOT_y**

	M_n	M_w	PDI
PBN ₁ DPOT ₉₉	18168	25764	1.42
PBN ₃ DPOT ₉₇	18639	26873	1.44
PBN ₅ DPOT ₉₅	21125	31889	1.51
PBN ₁₀ DPOT ₉₀	20353	29122	1.43

Table S3. Photophysics data of the **PBN_xDPOT_y**

	Absorption (nm)	Emission (nm)	FWHM (nm)	HOMO (eV)	LUMO (eV)	PLQY
PBN ₁ DPOT ₉₉	240	489	28	-5.99 eV	-2.40 eV	89.3%
PBN ₃ DPOT ₉₇	241	493	34	-5.98 eV	-2.48 eV	91.1%
PBN ₅ DPOT ₉₅	242	495	42	-5.96 eV	-3.05 eV	92.0%
PBN ₁₀ DPOT ₉₀	243	497	53	-5.97 eV	-2.84 eV	99.6%

Table S4. Photophysical data of **PBN₃DPOT_{97-z} w%** doped with host materials CzAcSF

PBN ₃ DPOT _{97-z} zw%: CzAcSF	$\phi_{PL}^{[a]}$ (%)	$k_r^{[b]}$ (s ⁻¹)	$k_{nr}^{[c]}$ (s ⁻¹)	$k_{ISC}^{[d]}$ (s ⁻¹)	$k_{RISC}^{[e]}$ (s ⁻¹)	$\tau_{PF}^{[f]}$ (s)	$\tau_{DF}^{[g]}$ (s)	Emission (nm)	FWHM (nm)
PBN ₃ DPOT ₉₇₋ 1w%: CzAcSF	89.25	1.38×10 ⁵	1.66×10 ⁴	3.95×10 ⁷	2.76×10 ⁷	2.52×10 ⁻⁸	9.31×10 ⁻⁶	488	51
PBN ₃ DPOT ₉₇₋ 5w%: CzAcSF	91.07	1.50×10 ⁵	1.47×10 ⁴	4.84×10 ⁷	3.02×10 ⁷	2.06×10 ⁻⁸	9.72×10 ⁻⁶	489	37
PBN ₃ DPOT ₉₇₋ 10w%: CzAcSF	99.61	1.88×10 ⁵	7.36×10 ²	7.02×10 ⁷	3.98×10 ⁷	1.87×10 ⁻⁸	9.44×10 ⁻⁶	490	35
PBN ₃ DPOT ₉₇₋ 15w%: CzAcSF	91.96	1.52×10 ⁵	1.33×10 ⁴	5.34×10 ⁷	3.44×10 ⁷	1.42×10 ⁻⁸	9.37×10 ⁻⁶	491	37

[a] Fluorescence quantum yield [b] Radiative transition rate [c] Non-radiative transition rate [d] gap-crossing rate [e] Reverse gap-crossing rate [f] PF lifetime [g] DF lifetime.

7. EL performance of PBN_xDPOT_y-z w%

Table S5. EL performance of PBN_xDPOT_y emitters

Polymer	z (w%)	J ^[a] (V)	L _{max} ^[b] (cd m ⁻²)	η ^[c]			FWHM (nm)	λ _{EL} (nm) / CIE (x, y) ^[d]
				η _{CE} (cd A ⁻¹)	η _{PE} (lm /W)	η _{EQE} (%)		
PBN ₁ DPOT ₉₉	1	4.0, 5.2, -	219.1	3.6, 3.0, 1.6	4.8, 3.0, 1.0	3.1, 2.0, 0.8	68	488/(0.19, 0.38)
	5	4.2, 5.1, -	303.3	4.5, 3.8, 2.4	3.7, 3.0, 1.5	2.3, 1.9, 1.2	70	488/(0.18, 0.36)
	10	4.4, 5.5, -	209.4	19.3, 13.5, 7.7	15.1, 10.0, 4.5	10.9, 6.9, 3.6	71	489/(0.17, 0.33)
	15	4.2, 5.4, -	307.2	7.7, 6.5, 6.2	4.8, 4.8, 3.8	3.6, 3.2, 3.0	73	488/(0.18, 0.34)
PBN ₅ DPOT ₉₅	1	3.9, 4.7, -	381.9	7.3, 4.6, 2.8	6.2, 3.5, 1.7	4.0, 2.9, 1.9	37	492/(0.15, 0.41)
	5	4.0, 4.8, -	426.3	8.0, 6.3, 3.4	4.9, 4.0, 4.2	4.5, 2.7, 1.6	39	492/(0.14, 0.40)
	10	4.5, 5.5, -	365.4	22.3, 19.6, 11.3	17.5, 13.6, 6.5	13.5, 10.4, 5.3	40	493/(0.15, 0.36)
	15	4.2, 4.9, -	482.0	6.0, 5.4, 7.6	6.7, 5.0, 4.5	4.1, 3.5, 2.1	42	492/(0.15, 0.37)
PBN ₁₀ DPOT ₉₀	1	4.2, 4.9, -	475.5	5.3, 4.6, 5.2	3.4, 2.9, 2.7	2.9, 2.5, 1.7	36	493/(0.18, 0.41)
	5	4.4, 5.1, 6.4	633.7	16.2, 3.7, 10.4	12.7, 8.5, 6.3	9.0, 6.6, 5.0	37	493/(0.13, 0.44)
	10	4.6, 5.4, 7.0	525.6	18.7, 17.3, 12.5	11.7, 11.6, 7.4	9.7, 8.8, 5.6	38	494/(0.14, 0.39)
	15	4.5, 5.0, 6.5	638.7	18.4, 15.2, 16.4	11.6, 10.6, 10.2	8.8, 8.0, 7.6	40	494/(0.14, 0.41)

^[a] At 10, 100 and 500 cd m⁻²; ^[b] Maximum brightness; ^[c] The maximum EL efficiency at 10 and 100 cd m⁻²; ^[d] Emission peaks and CIE color coordinates at 100 cd m⁻²

Table S6. Representative MR-TADF polymers with EQE and FWHM data since 2021

	EQE (%)	FWHM (nm)
D20	15.7	48
P10	19.4	38
PCzBN3	17.5	34
PCzTBN3	15.0	44
PCzDBN3	17.9	28
PAC-BSS	13.1	31
PBN ₃ DPOT ₉₇	12.0	39

8. References

- [1] A.D. Becke, Density-functional thermochemistry. III. The role of exact exchange, *J. Chem. Phys.* 1993, **98**, 5648–5652.
- [2] C. Lee, W. Yang, R.G. Parr, Development of the Colle-Salvetti correlation-energy formula into a functional of the electron density, *Phys. Rev. B* 1988, **37**, 785–789.
- [3] M.J. Frisch, G.W. Trucks, H.B. Schlegel, G.E. Scuseria, M.A. Robb, J.R. Cheeseman, G. Scalmani, V. Barone, B. Mennucci, G.A. Petersson, H. Nakatsuji, M. Caricato, X. Li, H.P. Hratchian, A.F. Izmaylov, J. Bloino, G. Zheng, J.L. Sonnenberg, M. Hada, M. Ehara, K. Toyota, R. Fukuda, J. Hasegawa, M. Ishida, T. Nakajima, Y. Honda, O. Kitao, H. Nakai, T. Vreven, J.A. Montgomery, J.E. Peralta, F. Ogliaro, M. Bearpark, J.J. Heyd, E. Brothers, K.N. Kudin, V.N. Staroverov, R. Kobayashi, J. Normand, K. Raghavachari, A. Rendell, J.C. Burant, S.S. Iyengar, J. Tomasi, M. Cossi, N. Rega, J.M. Millam, M. Klene, J.E. Knox, J.B. Cross, V. Bakken, C. Adamo, J. Jaramillo, R. Gomperts, R.E. Stratmann, O. Yazyev, A.J. Austin, R. Cammi, C. Pomelli, J.W. Ochterski, R.L. Martin, K. Morokuma, V.G. Zakrzewski, G.A. Voth, P. Salvador, J.J. Dannenberg, S. Dapprich, A.D. Daniels, Ö. Farkas, J.B. Foresman, J.V. Ortiz, J. Cioslowski, D.J. Fox, Gaussian 09, Gaussian, Inc., Wallingford CT, USA, 2009.